Comparative Analyses Based on Field-Measured Module Temperatures from a Utility-Scale Floating Photovoltaic System

Renzo Vargas, Givaldo dos Reis, Rodrigo P. Maruyama, Alex Manito, Marcelo Pinho Almeida, Roberto Zilles

University of São Paulo, São Paulo (Brazil)

Abstract

This study presents two analyses based on field measurements of module-temperature from a 5 MW floating photovoltaic (FPV) power plant and from a ground-mounted reference system. First, we assess five FPV modules strategically distributed across the array to quantify spatial variation in water-mediated cooling. Second, we compare FPV and ground-mounted reference modules–both monofacial and bifacial–to estimate the FPV-induced energy-yield benefit. Results show that the bifacial module exhibits the lowest median temperature among all modules analyzed; among monofacial units, the innermost FPV module has the lowest median temperature. Moreover, on a high irradiance day, the FPV–to–ground temperature difference remains below 10°C for 95.17% (bifacial) and 96.55% (monofacial) of the monitoring period, indicating a modest yet persistent thermal advantage for the floating photovoltaic installation.

Keywords: floating photovoltaics, module temperature, water-mediated cooling, monofacial and bifacial modules, thermal performance, energy-yield benefit, utility-scale photovoltaic system

1. Introduction

Rapid growth in solar deployment has sharpened land-use trade-offs with agriculture, urban development, and ecological functions (Turnley *et al.*, 2024; Manito *et al.*, 2026). Floating photovoltaics (FPV)—PV arrays installed on reservoirs, lakes, or irrigation basins—offer a way to ease these constraints (Niccolai *et al.*, 2024). By repurposing largely idle water surfaces, FPV both conserves terrestrial area and provides co-benefits including (Lamers *et al.*, 2018; Cuce *et al.*, 2022; Micheli, 2022; C.J. *et al.*, 2024; Garrod *et al.*, 2024; Koondhar *et al.*, 2024): (1) water-mediated cooling that limits temperature-driven efficiency losses; (2) decreases in reservoir evaporation; and (3) greater resource diversity in power systems with rising shares of variable renewables.

Module temperature is one of the most influential parameters governing PV performance (Hasan *et al.*, 2022). For crystalline-silicon modules, power output typically declines by 0.3–0.5 % for every 1 °C rise above standard test conditions (STC), so any technology that restrains thermal build-up can improve energy yield. Numerous laboratory and pilot-scale studies report that FPV modules operate several degrees cooler than ground-mounted counterparts (Dörenkämper *et al.*, 2021; K and K, 2024), crediting enhanced convective and evaporative heat transfer at the air–water interface. However, most of these investigations focus on small installations—often below 500 kW—or rely heavily on numerical models that have not been verified by long-term field data.

Utility-scale FPV projects (> 1 MW) introduce additional complexities, including larger hydrodynamic footprints, more pronounced spatial temperature gradients, and operational constraints associated with grid integration. Comprehensive, data-driven comparisons between such large FPV plants and ground-mounted PV systems are still rare. The present work addresses these gaps by conducting in-situ evaluation of module temperatures in a 5 MW FPV facility and a ground-mounted reference system.

1.1. Cooling effect above a water surface

The operating temperature of a PV module depends on incident irradiance, ambient conditions, wind characteristics, and the thermal properties of the PV cells. These variables behave quite differently when the array is installed on water rather than on solid ground or a roof. Several physical processes combine to keep the air—and thus the modules—cooler above a water surface:

- Subsurface solar penetration. Because water is largely transparent, part of the incoming solar flux passes

10.18086/swc.2025.03.12 Available at http://proceedings.ises.org

beneath the surface instead of being absorbed right at the interface, so the water layer that actually contacts the modules stays comparatively cool.

- Energy partitioning toward evaporation. On land or rooftops, most net radiation ends up as sensible heat that warms nearby surfaces and air. Over water, a substantial fraction is converted to latent heat that drives evaporation, limiting temperature rise.
- Vertical mixing. Water can circulate freely; the warmed upper layer mixes with deeper, cooler water, a heat-dissipation pathway unavailable to solid substrates.
- High heat capacity. Water's large specific heat dampens temperature fluctuations, keeping the boundary-layer air cooler than the air above soil or typical building materials.

The electrical performance of a PV module hinges strongly on the temperature of its solar cells. That is, a cooler module yields higher efficiency.

1.2. Objectives

This study pursues two complementary objectives: first, to characterize the spatial thermal behavior of the PV modules within a 5 MW utility-scale FPV system; and second, to benchmark the operating-temperature profiles of FPV modules against ground-mounted modules, providing a direct assessment of the net thermal advantage offered by deployment over water.

2. Field tests

2.1. Floating photovoltaic system

The study site is a 7.5-hectare floating photovoltaic (FPV) plant on a reservoir in a humid subtropical urban region, comprising 8,820 monofacial and 1,680 bifacial monocrystalline-silicon modules. The array is mounted on polyethylene pontoons with inter-row access walkways in an open layout; all modules are north-oriented at a fixed tilt of 12°. The plant is grid-connected. The module temperature coefficient is $\gamma = -0.34\%\ °C^{-1}$. To capture potential spatial temperature gradients, five representative modules (four monofacial and one bifacial) are instrumented with PT-100 resistance temperature detectors bonded to the rear surface of each module. Each sensor is connected to a datalogger that communicates via an infrared (IR) link for data retrieval and device configuration.

2.2 Ground-based photovoltaic reference system

The ground-mounted reference system is located approximately 17 km inland from the FPV site and comprises three PV modules—two monofacial and one bifacial—mounted on an open-rack support structure. The system is grid-connected. PT-100 resistance temperature detectors, bonded to the rear surface of each module, monitor module operating temperature and feed a datalogger identical to those used at the FPV site, ensuring consistent instrumentation. The modules are identical to those on the FPV plant and are oriented towards north at a fixed tilt of 23°.

3. Results

Module temperature data for the FPV plant were recorded continuously from August 2024 through July 2025. Only consistent datasets were retained for analysis. Each datalogger sampled the rear-surface temperature every 30 seconds; after ten samples, it computed the mean value and stored it as a single, 5-minute data record in non-volatile memory. Following the recommendation in (Dörenkämper *et al.*, 2021), comparisons were restricted to periods when POA irradiance at the FPV site exceeded 500 W/m^2. Results are organized into two cases:

- Case I: Field-measured module temperatures at five locations across the FPV system.
- Case II: Comparison of floating- and ground-mounted module temperatures under two irradiance regimes– Scenario 1 (clear, high-irradiance day), and Scenario 2 (overcast, low-irradiance day).

3.1. Case I: Field-measured module temperature in the floating photovoltaic system

For this case, Figure 1 shows the locations of the five PV modules instrumented for temperature monitoring.

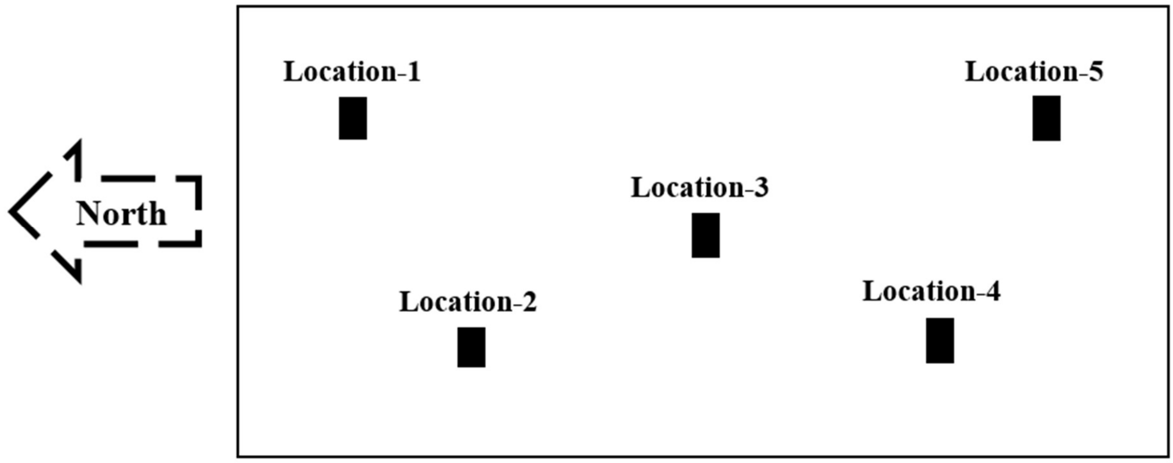

Figure 1: Location of the five modules under analysis within the FPV system.

In Figure 1, the modules at Locations 1–4 are monofacial, whereas the module at Location-5 is bifacial. Locations 1 and 5 are closer to open water; Location 2 and 4 are closer to land; Location 3 lies near the center of the FPV plant. Figure 2 presents a box plot summarizing their recorded temperatures.

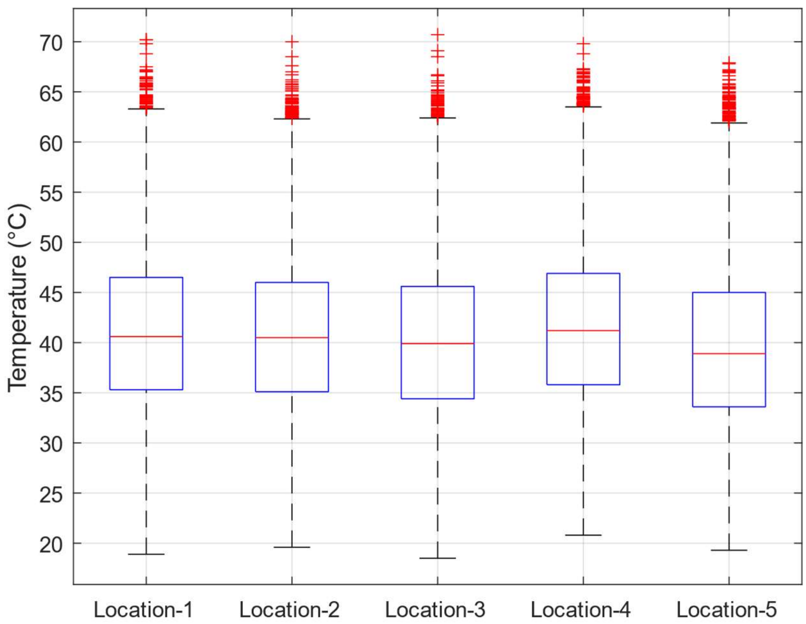

Figure 2: Boxplot of measured module temperatures at five different locations of the floating photovoltaic system

As shown in Figure 2, the median temperatures for modules 1-5 are 41.22 °C, 40.91 °C, 40.40 °C, 41.71 °C, and 39.72 °C, respectively. The maximum recorded temperatures are 70.20 °C, 70.00 °C, 70.70 °C, 69.80 °C, and 67.90 °C for modules 1-5, respectively.

After analyzing the Case I results, the following points emerge:

- Bifacial vs monofacial: Figure 2 shows that the bifacial module at Location-5 has a lower median temperature than the four monofacial modules at Locations 1-4. The temperature difference between the Location-5 module and those at Locations 1-4 are 2.30 °C, 2.10 °C, 2,80 °C, and 1.90 °C, respectively. Two factors likely contribute: (i) under comparable irradiance and ambient conditions, bifacial glass-glass modules dissipate heat more effectively through both faces, offsetting any extra heat from rear-side irradiance–particularly given the low albedo typical of FPV sites (Niccolai *et al.*, 2024); and (ii) greater wind exposure and a larger sky-view factor at Location-5 enhance forced and radiative cooling (Micheli, 2022).

- Within monofacial modules: The innermost monofacial module (Location-3) exhibits a slightly lower median temperature than the others–by 0.82 °C, 0.51 °C, and 1.30 °C relative to Locations 1, 2, and 4, respectively. These differences are negligible and likely reflect instrument sensitivity rather than a systematic effect. For practical purposes, the modules at Locations 1–4 can be considered to have the same median temperature.

- Extremes: Although Location-3 (monofacial) has the lowest median temperature among monofacial modules, it also registers the highest maximum temperature (70.7 °C). In contrast, the bifacial module at Location-5 records the lowest maximum temperature (67.9 °C).

3.2. Case II: Comparative module-temperature analysis of floating- and ground-mounted PV systems

In this subsection, two days representing distinct irradiance regimes are examined.

a) Scenario 1–clear, high-irradiance day

A day with approximately 6.43 kWh m⁻² of daily irradiation is selected. Analyses are presented for monofacial and bifacial modules.

a.1) Monofacial

Figure 3 shows the time series of module temperature at Location-3 of the FPV array—which exhibits the lowest median temperature among monofacial modules—alongside the ground-mounted reference (GMR) module. Figure 4 summarizes the distribution of the temperature differential ($\Delta T = T_{GMR} - T_{FPV}$) using 5-minute data between 06:00 and 18:00, reporting the proportions of intervals with $\Delta T \leq 10°C, 7°C,$ and $5°C$.

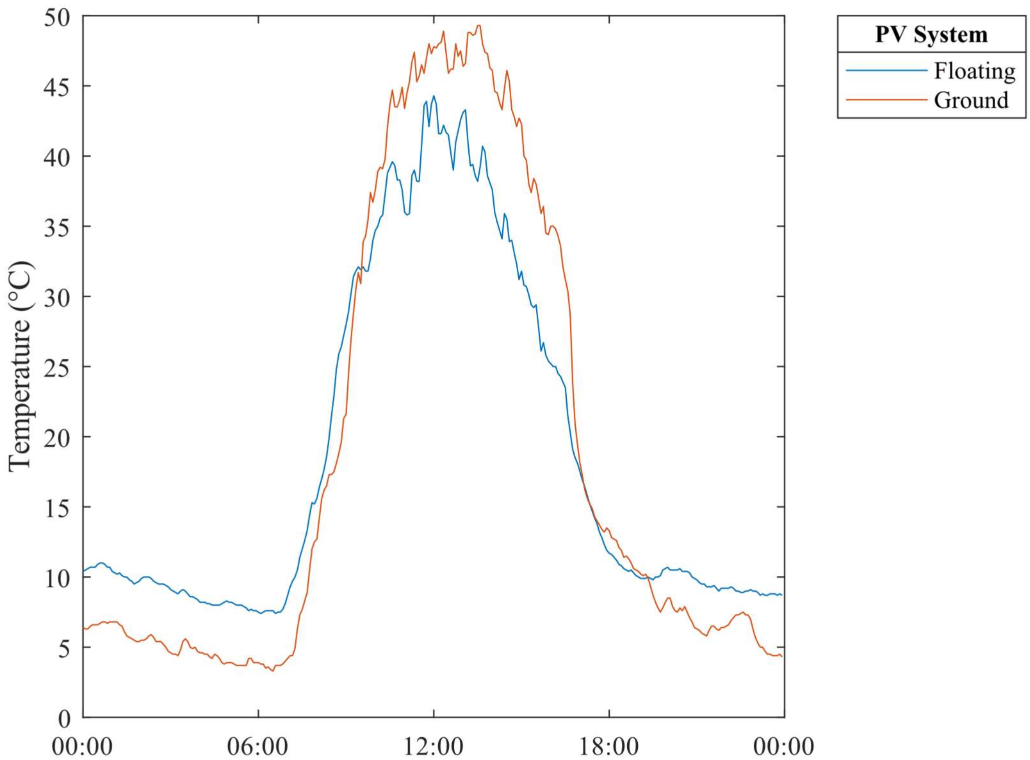

Figure 3: Temperature comparison between floating and ground-mounted monofacial PV module on a high irradiance day

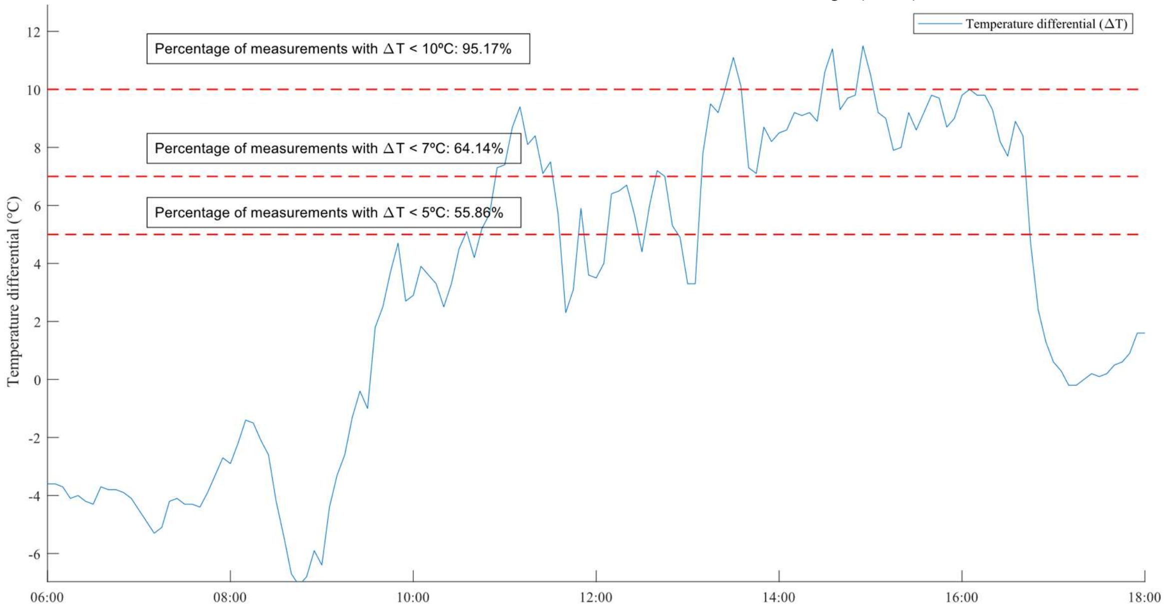

Figure 4: Temperature differential between floating and ground-mounted monofacial PV modules on a high irradiance day

Key finds (monofacial, Scenario 1):

- The maximum differential in Figure 3 is 11.50 °C, recorded at 14:55, an isolated peak not sustained throughout the afternoon.
- As shown in Figure 4, $\Delta T \leq 10°C$ for 95.17 % of 5-minute intervals. Using a temperature coefficient of power $\gamma = -0.34$ % $°C^{-1}$, this places an upper bound of ~3.4% on the FPV temperature-driven power advantage during 95.17% of the monitored daylight period. Analogous bounds follow for the 7 °C and 5 °C threshold.

a.2) Bifacial

Figure 5 presents the time series of module temperature at Location-5 on the FPV array alongside the bifacial GMR module. Figure 6 summarizes the distribution of $\Delta T = T_{GMR} - T_{FPV}$, using 5-minute samples between 06:00 and 18:00, and reports the proportion of intervals with $\Delta T \leq 10°C, 7°C,$ and $5°C$.

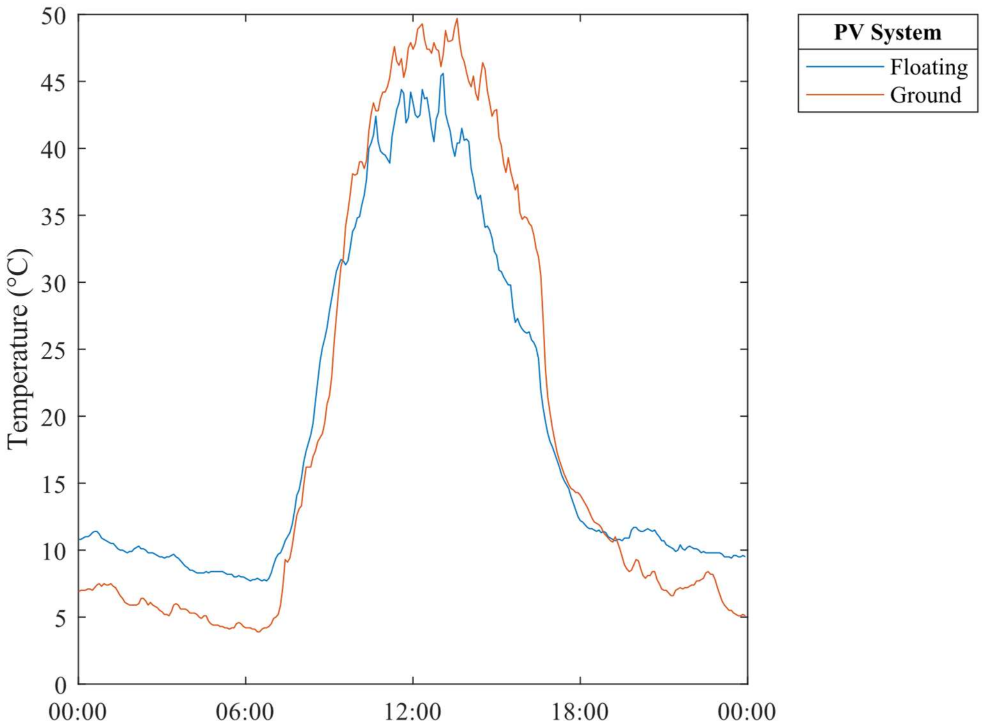

Figure 5: Temperature comparison between floating and ground-mounted bifacial PV module on a high irradiance day

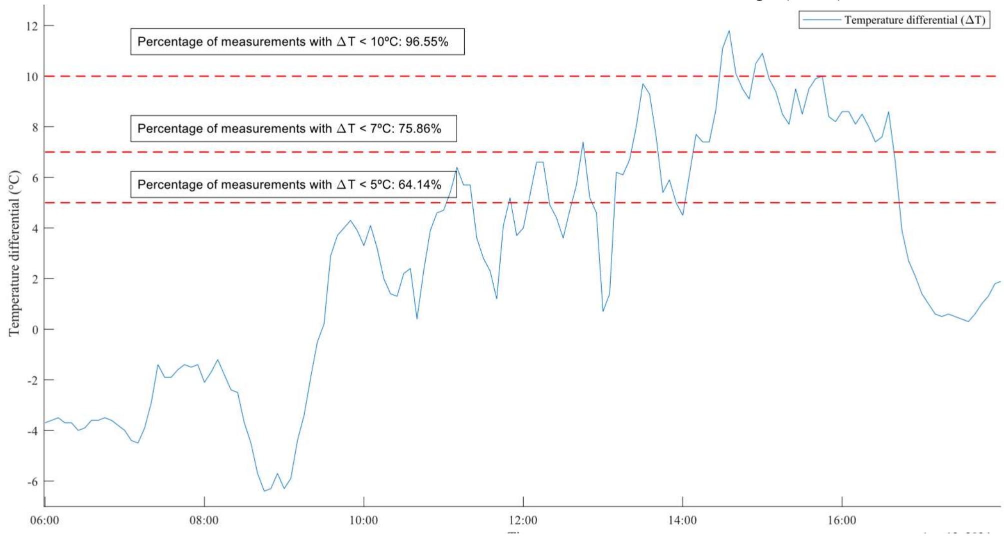

Figure 6: Temperature differential between floating and ground-mounted bifacial PV modules on a high irradiance day.

Key findings (bifacial, Scenario 1):

- The largest differential in Figure 5 is 11.80 °C at 14:35, a temporal peak not sustained later in the day.
- From Figure 6, $\Delta T \leq 10°C$ for 96.55 % of the 5-minute samples. With γ = −0.34 % °C^{-1}, this implies an FPV temperature-driven power benefit bounded above by ∼3.4% for 96.55% of daylight intervals. Comparable bounds apply for the 7 °C and 5 °C thresholds.

b) Scenario 2–overcast, low-irradiance day

A day with approximately 2.60 kWh m^{-2} of daily irradiation is selected. Analyses are presented for monofacial and bifacial modules.

b.1) Monofacial

Figure 7 displays temperature traces for the FPV module at Location-3 and the monofacial GMR module. Figure 8 presents the distribution of $\Delta T = T_{GMR} - T_{FPV}$ based on 5-minute data collected between 06:00 and 18:00, indicating the proportion of intervals with $\Delta T \leq 10°C, 7°C,$ and 5°C.

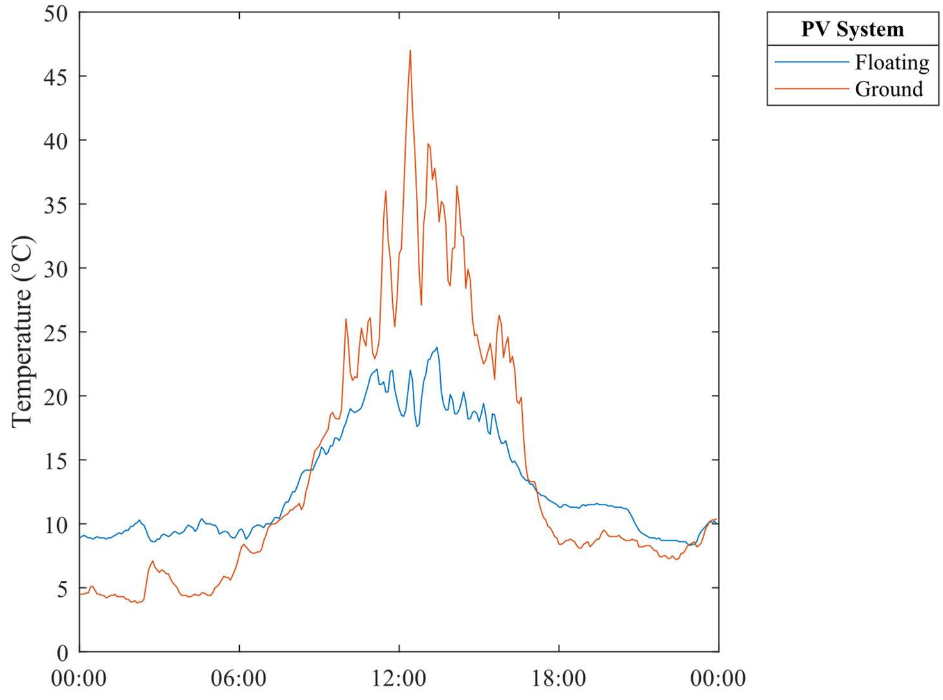

Figure 7: Temperature comparison between floating and ground-mounted monofacial PV module on a low irradiance day

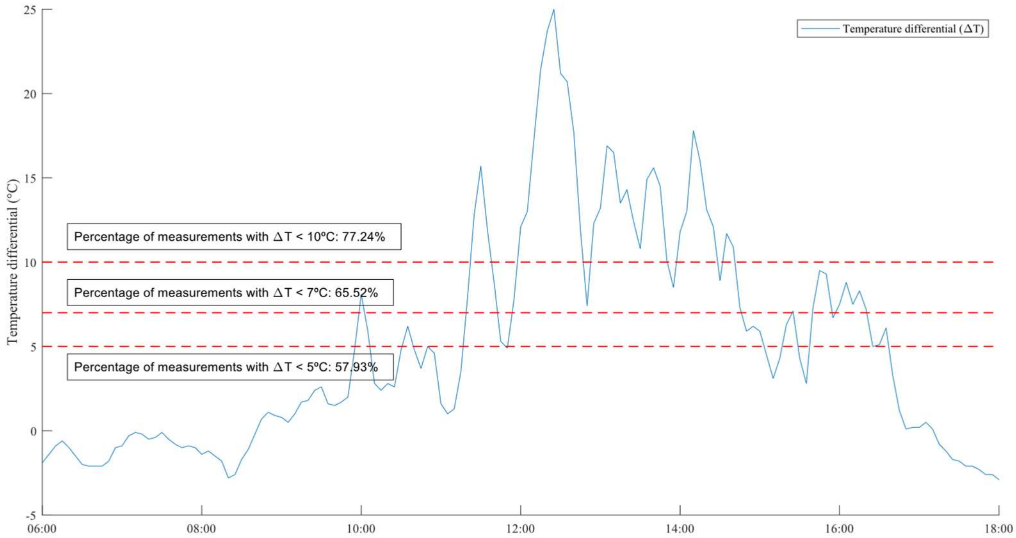

Figure 8: Temperature differential between floating and ground-mounted-monofacial PV modules on a low irradiance day.

Scenario 2–monofacial summary:

- Figure 7 shows a maximum ΔT of 25 °C at 12:25; this is an isolated event rather than a sustained afternoon pattern.
- As indicated in Figure 8, 77.24% of 5-minute intervals satisfy $\Delta T \leq 10$℃. Using γ = −0.34 % °C⁻¹, the corresponding upper bound on the FPV temperature-related power gain is ∼3.4% over that share of the period. Similar limits apply for the 7 °C and 5 °C cutoffs.

b.2) Bifacial

In Figure 9, module-temperature times series for the FPV module at Location 5 are compared with those of the bifacial GMR module. Figure 10 summarizes the distribution of $\Delta T = T_{GMR} - T_{FPV}$ at 5-minute resolution between 06:00 and 18:00, highlighting the shares of intervals at or below 10℃, 7℃, and 5℃.

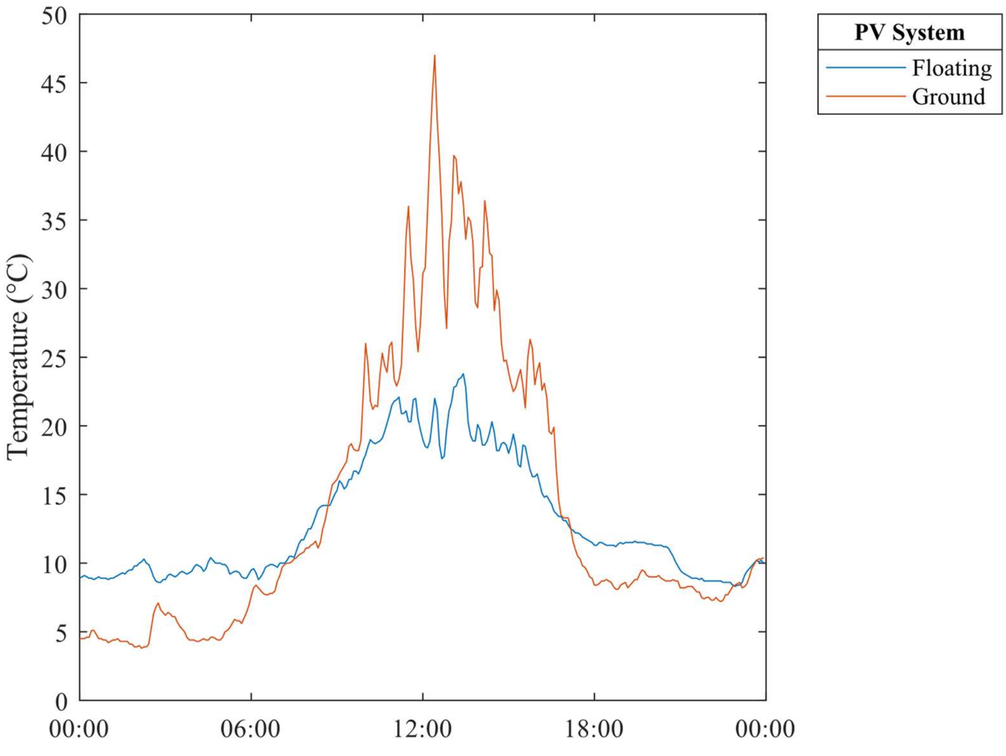

Figure 9: Temperature comparison between floating and ground-mounted monofacial PV module on a low irradiance day

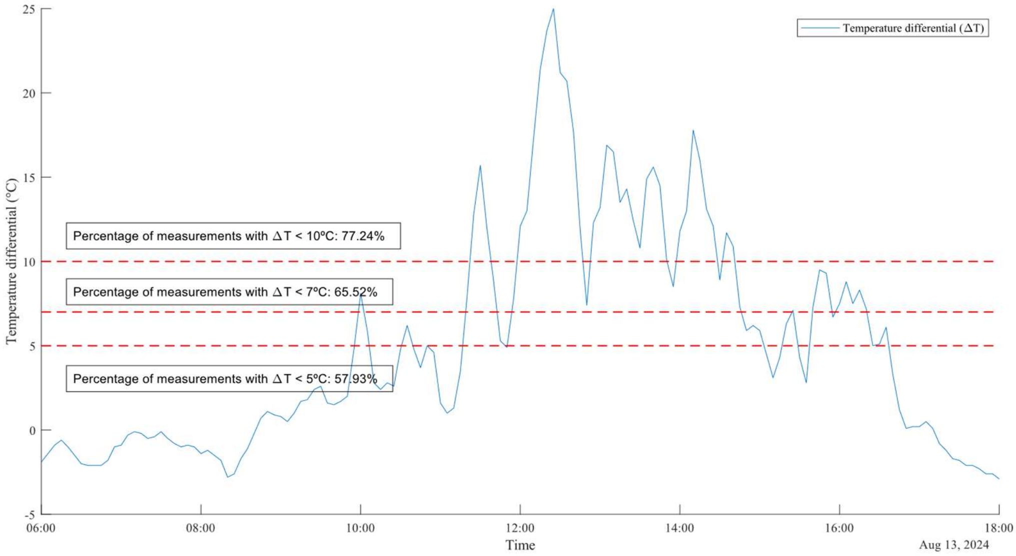

Figure 10: Temperature differential between floating and ground-mounted monofacial PV modules on a low irradiance day.

Highlights (bifacial, Scenario 2):

- Peak differential: 25.50 °C at 12:25 (Figure 9).
- $\Delta T \leq 10$℃ for 77.24 % of 5-minute observations (Figure 10). With $\gamma = -0.34$ % $°C^{-1}$, this constrains the FPV temperature-driven advantage to $\leq \sim$3.4% across that fraction of the day; analogous estimates hold for the 7 °C and 5 °C limits.

4. Discussion

In Case I, the bifacial module exhibits the lowest median temperature among all units. Among the monofacial modules, the unit closest to the center of the FPV array shows the lowest median temperature, whereas perimeter modules are consistently warmer. This pattern contrasts with other studies (Dörenkämper *et al.*, 2021), which reported the coolest temperatures at the array edge. However, the differences in monofacial median temperatures within the FPV array are sufficiently small to be considered negligible; for practical purposes, Locations 1-4 have essentially the same median temperature. In Case II, the temperature differential between the FPV modules and the ground-mounted reference indicates that the FPV-related energy-yield advantage rarely exceeded 3.4 % over the monitoring period. By contrast, other studies have reported substantially higher gains (Niccolai *et al.*, 2024), likely reflecting differences in weather regimes, albedo, and other environmental conditions.

5. Conclusions

This work presented two complementary analyses based on a year-long dataset of field-measured photovoltaic (PV) module temperatures from a 5 MW utility-scale floating PV (FPV) plant and a ground-mounted reference system. In the first analysis, we compared five modules strategically distributed across the FPV array; the bifacial module exhibited the lowest median temperature, while the monofacial modules showed approximately the same median temperature. In the second analysis, on representative high- and low-irradiance days, the temperature differences between the FPV modules and the ground-mounted reference indicate that the FPV-related energy-yield gain is unlikely to exceed 3.4%. Future work will extend the monitoring horizon and incorporate additional environmental variables.

6. Acknowledgments

This work was supported by the São Paulo Research Foundation (FAPESP), under grants #2023/00597-9, and #2023/17658-0, and carried out within the scope of the activities of the National Institute for Technological Development of Photovoltaic Solar Energy Applications, INCT-DAESF, CNPq/MCTI/Brazil, Process 408486/2024-

4. We gratefully acknowledge the technicians and researchers of the Photovoltaic Systems Laboratory (LSF-IEE/USP) for their valuable support and the use of their infrastructure.

7. References

C.J., R. *et al.* (2024) 'Towards sustainable power generation: Recent advancements in floating photovoltaic technologies', *Renewable and Sustainable Energy Reviews*, 194(February), p. 114322. Available at: https://doi.org/10.1016/j.rser.2024.114322.

Cuce, E. *et al.* (2022) 'Floating PVs in terms of power generation, environmental aspects, market potential, and vhallenges', *Sustainability*, 14(5), p. 2626. Available at: https://doi.org/10.3390/su14052626.

Dörenkämper, M. *et al.* (2021) 'The cooling effect of floating PV in two different climate zones: A comparison of field test data from the Netherlands and Singapore', *Solar Energy*, 214(November 2020), pp. 239–247. Available at: https://doi.org/10.1016/j.solener.2020.11.029.

Garrod, A. *et al.* (2024) 'An assessment of floating photovoltaic systems and energy storage methods: A comprehensive review', *Results in Engineering*, 21(December 2023), p. 101940. Available at: https://doi.org/10.1016/j.rineng.2024.101940.

Hasan, K. *et al.* (2022) 'Effects of different environmental and operational factors on the PV performance: A comprehensive review', *Energy Science & Engineering*, 10(2), pp. 656–675. Available at: https://doi.org/10.1002/ese3.1043.

K, A. and K, V. (2024) 'A comparative study of floating and ground-mounted photovoltaic power generation in Indian contexts', *Cleaner Energy Systems*, 9(January), p. 100140. Available at: https://doi.org/10.1016/j.cles.2024.100140.

Koondhar, M.A. *et al.* (2024) 'Reviewing floating photovoltaic (FPV) technology for solar energy generation', *Energy Strategy Reviews*, 54(March), p. 101449. Available at: https://doi.org/10.1016/j.esr.2024.101449.

Lamers, M.W.P.E. *et al.* (2018) 'Temperature effects of bifacial modules: Hotter or cooler?', *Solar Energy Materials and Solar Cells*, 185(March), pp. 192–197. Available at: https://doi.org/10.1016/j.solmat.2018.05.033.

Manito, A.R.A. *et al.* (2026) 'What to expect from agrivoltaic systems? A comprehensive review of experimental findings and field applications', *Renewable and Sustainable Energy Reviews*, 225(July 2025), p. 116137. Available at: https://doi.org/10.1016/j.rser.2025.116137.

Micheli, L. (2022) 'The temperature of floating photovoltaics: Case studies, models and recent findings', *Solar Energy*, 242(March), pp. 234–245. Available at: https://doi.org/10.1016/j.solener.2022.06.039.

Niccolai, A. *et al.* (2024) 'A review of floating PV systems with a techno-economic analysis', *IEEE Journal of Photovoltaics*, 14(1), pp. 23–34. Available at: https://doi.org/10.1109/JPHOTOV.2023.3319601.

Turnley, J.W. *et al.* (2024) 'The viability of photovoltaics on agricultural land: Can PV solve the food vs fuel debate?', *Journal of Cleaner Production*, 469(January), p. 143191. Available at: https://doi.org/10.1016/j.jclepro.2024.143191.